Investigation of the Structure and the Plasma Parameters in a "Critical Velocity" Rotating Plasma

G. Himmel, E. Möbius, and A. Piel

Ruhr-Universität Bochum, Institut für Experimentalphysik II

(Z. Naturforsch. **31 a**, 934–941 [1976]; received June 29, 1976)

The structure and the plasma parameters of a rotating plasma showing Alfvén's critical velocity were investigated for the first time by means of Langmuir probes. It was demonstrated that the occurrence of the critical velocity is causally connected with the formation of a spoke structure. The electron temperature and the plasma density were determined with local resolution by which a detailed balance concerning the plasma density and the current transport became possible. The importance of turbulent electron heating for rapid ionization at the critical velocity is emphasized. In this process the modified two-stream-instability obviously plays an outstanding role.

Introduction

The voltage limitation in crossed-field discharges has been reported by several authors [1, 2]. This observation is commonly attributed to a limitation of the relative velocity between a magnetized plasma and the neutral gas to a value, which is generally known as "critical velocity". This effect was proposed by Alfvén [3] in connection with his theory on the origin of the solar system, which gives a surprisingly good description of some astrophysical phenomena. Alfvén's hypothesis essentially predicts a rapid ionization of the neutral gas as soon as the relative motion between plasma and gas exceeds the critical velocity.

In a recent article Danielsson [4] has proved the collisionless nature of this gas-plasma interaction. An outstanding result of his plasma-gas-impact experiment is the demonstration of the connection between the braking of the plasma motion and a strong electron heating.

Among several models [5] which try to explain the critical velocity phenomenon the most successful in the light of recent experiments have turned out to be those which involve collective effects such as turbulent electron heating by means of two-stream instabilities [6]. Nevertheless the critical velocity phenomenon is still far from being understood especially as the predictions of the models up to now were verifiable only by the results of macroscopic parameter studies.

In the present state of discussion it has become necessary to determine exactly the range of discharge parameters which is governed by this effect as well as to obtain reliable data about the plasma structure and its microscopic parameters such as electron temperature and density.

It is for this reason that the present article reports diagnostic measurements on a rotating plasma. The investigations were performed in a homopolar-experiment because of its simple geometry and quasi-stationary operation.

Reprint requests to A. Piel, Institut für Experimentalphysik, Universität Bochum, Postfach 21 48, Gebäude NB, 5/132, *D-4630 Bochum-Querenburg.*

I. The Discharge Parameters of the Rotating Plasma

The purpose of macroscopic measurements in the first chapter is on the one hand to prove the existence of the voltage limitation in the discharge under consideration and to confirm the results of Fahleson [1] and on the other hand to determine the limits of the parameter range over which the voltage limitation can be observed. By this means this special type of discharge may be separated from other crossed field discharges.

1. Device

The device corresponds to the homopolar described by Fahleson (Figure 1). The radial electric field is produced by concentric electrodes. An axial homogenous magnetic field is superimposed, with stationary field strengths up to 0.6 T. The discharge current is supplied by a capacitor bank (30 μF, 7 kV) and is adjusted by a variable resistor. Contrary to Fahleson's experiment a very large distance between the insulators and the electrodes has been chosen.

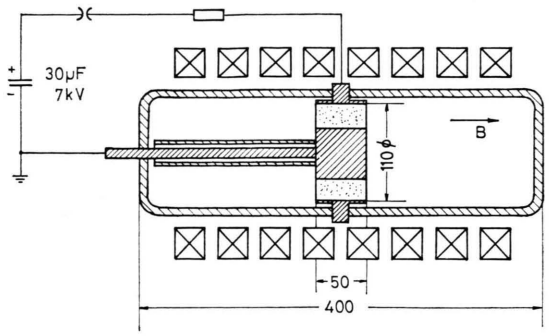

Fig. 1. Schematic diagram of the rotating plasma. The electrode system is contained in a long pyrex vacuum vessel in order to keep insulators far away from the discharge volume (dotted area).

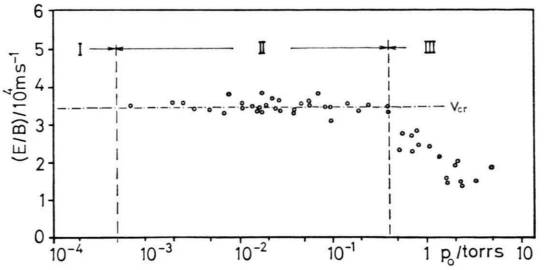

Fig. 2. E/B-velocity derived from the burning voltage vs. gas pressure. The dot-dash line represents Alfvén's critical velocity v_{cr}.

2. *Voltage Limitation Measurements*

The burning voltage of the discharge is linearly dependent on the magnetic field strength according to the relation

$$U_D = v_{cr} B (r_o - r_i) \qquad (1.1)$$

as described by Fahleson. r_o, r_i are the radii of the outer and inner electrodes respectively. Within a wide range of parameters the velocity v_{cr} for various gases agrees with Alfvén's critical velocity [7], which is connected to the mass m_i and the ionization potential W_i of the used gas by the condition

$$(m_i/2) v_{cr}^2 = W_i . \qquad (1.2)$$

All the further investigations described in this paper have been performed in Helium. The voltage limited stage of the discharge can be maintained for as long as 1 ms. Because of this fact investigation of the parameters will be much more promising in this device.

For discharge currents from 10 A to 10000 A no significant variations of the burning voltage could be detected. Even for the highest currents the "burn out" of the neutral gas reported by Fahleson did not occur, a fact which would seem to be due to the large reservoir of gas in the device.

By varying the neutral gas pressure a lower and an upper value was found for the critical velocity (Fig. 2) and here three different pressure ranges must be distinguished. Range II from $5 \cdot 10^{-4}$ torrs up to $5 \cdot 10^{-1}$ torrs is marked by the critical velocity. Leaving range II towards range I the delayed ignition appears, which had been investigated earlier by Sherwood and Kunkel [8]. Within range I below $5 \cdot 10^{-4}$ torrs no self sustaining discharge could be set up even with preionization. Above $5 \cdot 10^{-1}$ torrs the burning voltage steadily falls below the critical value. Simultaneously the proportionality to the magnetic field is lost.

3. *The Macroscopic Structure of the Discharge*

We were able to show definitively that the given relation of the burning voltage to the discharge parameters was not due to electrode effects by conducting the following investigations:

1. Varying the distance of the electrodes by a factor of three relation (1.1) was confirmed.
2. Measuring the floating potential within the plasma with a radially movable probe a linear dependance of the potential could be found.

It was further shown that there was no trace of either a cathode sheath or an anode sheath.

Of course these measurements also show, that the homopolar discharge is by no means as homogeneous as supposed earlier [1]. Potential fluctuations on the time scale of a few microseconds could be detected. We attribute these fluctuations to a spoke structure of the discharge. Velocity measurements with two probes separated by a distance of two centimeters in azimuthal direction demonstrated that these spokes are moving with the critical velocity v_{cr}. Moreover the spoke structure could be detected on the light signal after having increased the spatial resolution up to 4 mm by a system of apertures. So the azimuthal structure turns out to be an essential aspect of this type of a rotating plasma and requires particular attention in the following investigations of the plasma parameters.

II. Investigations of the Microscopic Behaviour of the Plasma

A spatially resolved determination of the plasma density and the electron temperature can be effected in a simple manner by the use of Langmuir probes. Probe measurements in a rotating plasma have already been performed by Lehnert et alias [9]. But these have only been restricted to the boundary layer of a fully ionized plasma, whereas our measurements were obtained directly within the critically rotating plasma. Applying this approved technique to the described plasma requires some further development of the diagnostics with respect to the construction and methods.

1. Probe Circuit

The probe circuit is shown in Figure 3. Because of the large potential fluctuations a floating double probe technique is required. The probe voltage is supplied by a battery with a buffer capacitor. An inductive current probe with a bandwith of 10^3 to $5 \cdot 10^7$ Hz provides for the insulation of the current signal.

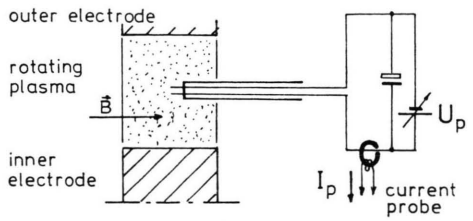

Fig. 3. Circuit diagram for floating double probes. An inductive current probe allows the probe current to be measured without electric connection to the floating probe.

The probes have been adapted to meet the various demands made upon them (Figure 4). The plasma density is calculated from the ion current of the symmetrical double probe according to Laframboise [10]. The probe diameter is small compared to the ion gyro radius, so the influence of the magnetic field on the ion current may be neglected.

With its front the asymmetrical double probe collects electrons parallel to the magnetic field. The electron temperature is determined from the electron retardation current. The large area-ratio of the probe $(F_2 : F_1 > (m_i/m_e)^{1/2})$ means that the electron current can be measured nearly up to the saturation point. Moreover edge-effects of plane probes are eliminated by the magnetic field.

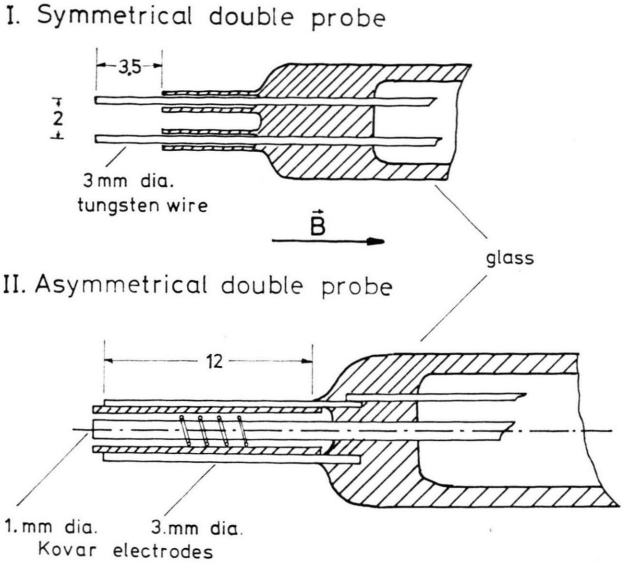

Fig. 4. Dimensional outline of the double probes.

2. Interpretation of the Probe Signal

Figure 5, which shows the probe current at a fixed probe voltage, proves the presence of high density spokes rotating in the discharge. Because of the azimuthal motion of the spokes the desired spatial resolution requires an adequate time resolution. For that reason the analysis of the probe signal was decisively improved in comparison with the time integrated method of Lehnert et al. [9], which only gives an average over the azimuthal structure.

The probe current gives a direct representation of the density structure as is shown below. Although the parameters vary on a time scale of a few micro-

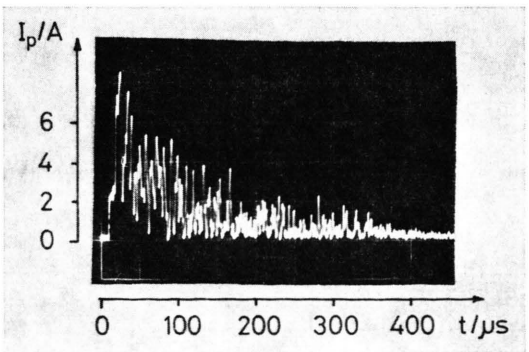

Fig. 5. Oscillographic trace of the probe signal. The existence of high density current spokes is evident. The peak density within the spokes decreases exponentially due to the decrease of the discharge current.

seconds, the use of electrostatic probes is justified due to the sheath formation time being very much shorter ($\omega_{pi}^{-1} \approx 10^{-8}$ s). However it is impossible to sweep the whole characteristics over a time period which is short compared with the time scale of the fluctuations. Therefore the probe characteristics have to be determined shot by shot. The determination of the electron temperature is restricted to the peak density of the current spokes. During one discharge the density in the spokes decreases exponentially due to the decrease of the discharge current. The initial value of the exponential which best approximates to decrease of the density yields the probe current. In this connection a constant electron temperature is assumed. The consistency of this assumption will be shown below. – A characteristics of the asymmetrical double probe constructed in the way described is presented in Figure 6. The error bars represent the standard deviation about the best approximating exponential for each point.

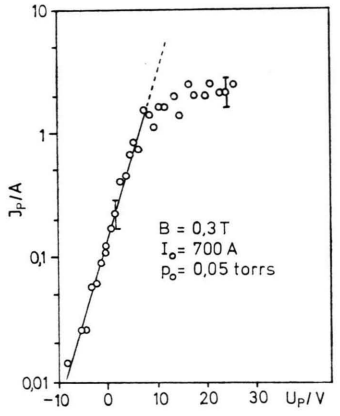

Fig. 6. Probe characteristics of the asymmetrical double probe. The exponential part of the characteristics yields an electron temperature of T_e=3.8 eV.

3. Electron Temperature

The electron temperature T_e is derived from the slope of the electron current in a semi-log plot, neglecting those points close to the plasma potential which may be influenced by the finite area ratio of the probe. T_e is found to be almost independent of the discharge parameters, the gas pressure, the magnetic field strength and the discharge current (Figure 7).

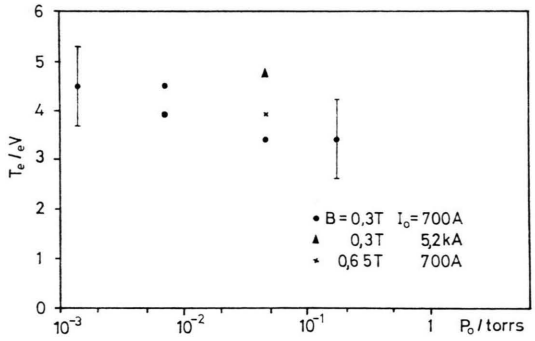

Fig. 7. Measured electron temperature for various discharge conditions.

4. Determination of the Plasma Density

Using this electron temperature the peak density in the current spokes can be calculated exactly. Within the other regions of the structure this value of T_e, though not exactly known, nevertheless may be used, for it is a particularity of a cylindrical probe that an inaccurately known electron temperature only causes small errors in the plasma density [11]. Therefore we feel justified in taking the value and shape of the density directly from the ion current of the symmetrical double probe. A typical shape of a current spoke is shown in Figure 8. Here we distinguish two regions:

1. a very steep increase of the density at the front of the spoke and
2. a smooth decrease in the rear.

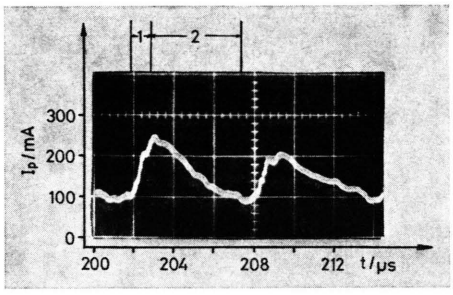

Fig. 8. Probe current representing the typical density profile of the current spokes. The spoke is characterized by a steep front (1) and a smooth decrease (2).

The density values calculated from the electron saturation current of the asymmetrical double probe were found to agree closely with the results obtained from the ion current. In addition they were supported by transmission measurements with 8 mm microwaves.

5. Shape and Parameter Variation of the Density

It can be seen from the axial density profile that the rotating plasma is restricted to a volume between the electrodes (Figure 9). The shape of this

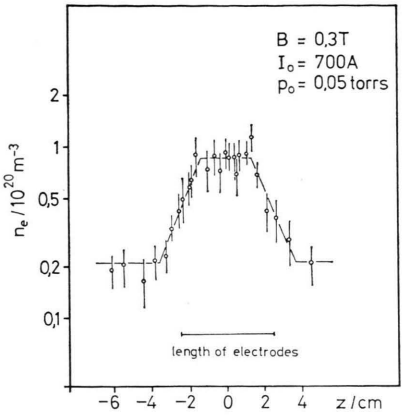

Fig. 9. Axial density profile. The discharge essentially is restricted to the length of the electrodes.

profile allows some conclusions to be drawn about the loss processes for charged particles. These will be discussed later in connection with a particle balance of the plasma.

A proportionality between electron density within the spokes and the discharge current was found by varying the initial current of the discharge (Figure 10). So the earlier assumption about the decrease of the density in time was proved to be valid.

No substantial variation of the density with the other discharge parameters such as magnetic field strength and neutral gas pressure could be detected.

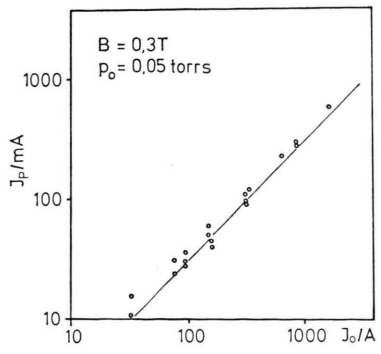

Fig. 10. Probe current vs. discharge current. The peak density of the current spokes turns out to depend linearly on the discharge current.

6. Magnetic Probe Measurements

In addition magnetic probes were used to investigate more closely the azimuthal structure of the rotating plasma, especially with respect to the current balance. By means of a magnetic probe with a maximum diameter of 4 mm the current distribution within the plasma could be determined with a sufficient spatial resolution. These measurements show that the discharge current is in fact restricted to the current spokes, which were already identified by the structure of the plasma density (Figure 11). A

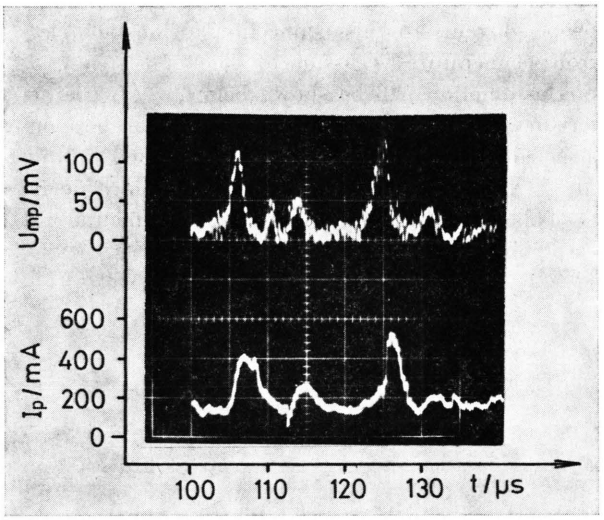

Fig. 11. Comparison of magnetic probe signal (upper trace) and density signal (lower trace). The current maximum corresponds to the high density part of the spokes.

knowledge of the current distribution, the total current and the burning voltage now allows the conductivity of the plasma to be calculated. This is important for a discussion of the current balance below.

III. Theory

The existing theories concerning the critical velocity phenomenon either restrict themselves to macroscopic properties like energy balance and momentum balance of the whole plasma [5, 12] or although based on microscopic models [13] they can only be tested with respect to their predictions about macroscopic properties like the burning voltage of the plasma. The measurements described in the present article allow for direct comparisons of microscopic model assumptions with similarly mi-

croscopic results. Subsequently the basic equations of a plasma model viz. the particle balance, current balance and heat balance of the electrons and the importance of the azimuthal structure will be discussed.

Particle Loss Mechanisms

A balance equation of the plasma density requires a consideration of the dominant mechanisms of the production and the loss of charged particles. Ionization by electron impact is regarded by all authors to be the most important process in plasma production. The problematical aspects are thus to be found in the unknown mechanism of electron heating.

Up to now ambipolar diffusion parallel to the magnetic field with wall recombination has been assumed to be the dominant loss mechanism [13]. But the shape of the measured axial density profile proves that this process is not important in the discharge under consideration. Such a shape might arise from diffusion with volume recombination in the outer region. However the loss rate cannot exceed the recombination rate. This rate can be overestimated using the recombination rates given by Bates, Kingston and McWhirter [14] at the measured temperature of $T_e = 3.8$ eV and a maximum density of $n_e = 10^{20}\,\mathrm{m}^{-3}$ resulting in a loss rate of $3.1 \cdot 10^{21}\,\mathrm{m}^{-3}\,\mathrm{s}^{-1}$ which is four orders of magnitude less than the loss rate due to the discharge current discussed subsequently.

Current Balance

For a current to flow radially a high mobility of the charged particles across the magnetic field is required. The importance of symmetrical resonant charge exchange collisions for the ion motion has been pointed out by Sherman [15]. The mean free path for charge exchange being small compared to the gyro radius, the ions essentially move in the radial direction. Using the mean radial velocity $\langle v_{ir} \rangle$ computed by Sherman and the measured electron density we obtain an ion current

$$j_i = n_e\, e\, \langle v_{ir} \rangle \tag{3.1}$$

which is comparable to the discharge current.

Sherman's model implies that a constant ion current is transported through the plasma. But there are no indications as to where these ions are produced. A consequence of this model would be the assumption of an anode sheath producing the ions, since no ions originate at the anode itself. A self-consistent calculation of such a sheath [16] leads to a large potential drop across the sheath which could not be observed experimentally.

The ion production thus takes place in the whole plasma volume. On the way from anode to cathode a gradual transition from electron to ion current must occur. These considerations lead to the Ansatz:

$$e\,S = \operatorname{div} j_i = -\operatorname{div} j_e \tag{3.2}$$

which expresses the balance between the ionization rate S and the loss due to the transport of charged particles by the current.

Integrating this relation over the plasma volume one obtains a mean loss rate R

$$R = \frac{1}{e}\frac{1}{V}\int \operatorname{div} j_i \,\mathrm{d}V \approx \frac{j_d}{e\,(r_o - r_i)} \tag{3.3}$$

amounting to $R = 2 \cdot 10^{25}\,\mathrm{m}^{-3}\,\mathrm{s}^{-1}$ at current density of $j_d = 10\,\mathrm{A/cm^2}$ and an electrode distance of $r_o - r_i = 3$ cm. The particle transport due to the discharge current thus represents the dominant loss mechanism.

Classical Electron Conductivity

The particle balance (3.2) requires a radial electron current of the same magnitude as the ion current. Within the pressure range $p_0 < 0.5$ torrs the electron-neutral collision frequency ν_{en} is small compared to the gyro frequency ω_{ce}. The electron conductivity

$$\sigma_e = \frac{e^2 n_e}{m_e}\frac{\nu_{en}}{\omega_{ce}^2} \tag{3.4}$$

at typical conditions: $n_e = 10^{20}\,\mathrm{m}^{-3}$, $p_0 = 0.05$ torrs, $B = 0.2$ T results in $\sigma_e = 0.34\,\mathrm{A/Vm}$ compared with the experimental value

$$\sigma_{exp} = j_d/E = 13\,\mathrm{A/Vm}\,.$$

Therefore electron-neutral collisions cannot explain the required electron current.

Coulomb collisions also turn out to be negligible since it is only in excess of a plasma density of $n_e = 5 \cdot 10^{20}\,\mathrm{m}^{-3}$ – corresponding to discharge currents of more than 10 kA – that the experimental conductivity is attained. So classical collision processes turn out to be unsuitable for explaining the required electron conductivity.

Classical Heat Balance

A further indication of the poor efficiency of classical collision processes arises from the heat balance of the electrons (Lehnert [13])

$$\boldsymbol{j}_e \boldsymbol{E} = 2\, n_e \varkappa_e(T_e)\, \nu_{en}\, k(T_e - T_n)\,. \qquad (3.5)$$

The heating by elastic collisions with neutrals is balanced by the heat loss in inelastic collisions, $\varkappa_e(T_e)$ being the fractional energy loss in a collision with a neutral. From (3.5) and

$$j_e = -n_e\, e\, \langle v_{er} \rangle = n_e\, e\, \frac{E}{B}\, \frac{\nu_{en}/\omega_{ce}}{1 + (\nu_{en}/\omega_{ce})^2} \qquad (3.6)$$

we obtain in the limit $\nu_{en} \ll \omega_{ce}\, T_e \gg T_n$ the relation:

$$\tfrac{1}{2}\, m_e (E/B)^2 = \varkappa_e(T_e)\, k\, T_e$$

which for constant E/B predicts a temperature T_e independent of the neutral gas pressure. The ionization rate by electron impact calculated using this temperature

$$S = n_e\, n_g\, \langle \sigma_i\, v_e \rangle$$

reaches at $p_0 \approx 0.5$ torrs the magnitude of the loss rate (3.3). The existence of E/B values below the critical velocity within pressure range III can be explained from a classical heat and current balance.

However the dependence of the ionization rate on the target density n_g leads within the pressure range II ($p_0 < 0.5$ torrs) to a rapidly increasing discrepancy in the particle balance, which at the lower limit $p_0 = 5 \cdot 10^{-4}$ torrs amounts to a factor of 10^3 by which the losses exceed the production of charged particles. The existence of the plasma present therefore requires high energy electrons which are responsible for the ionization but which cannot arise from the classical heating mechanism presented.

Electrostatic Microinstabilities

In crossed field discharges microinstabilities can arise which are driven by a relative drift between electrons and ion [17,18]. Because of their large growth rates the electrostatic instabilities i. e. the modified two stream instability, the ion acoustic instability and the beam cyclotron instability are most important.

Since the electrons essentially follow the $E \times B$ drift without collisions and, on the other hand, the ion motion is determined by charge exchange collisions, a relative drift comparable to the critical velocity occurs, which due to $k\, T_e < 2\, W_i$ by far exceeds the ion acoustic velocity.

By means of the turn-on conditions a choice between the three instabilities mentioned above becomes possible for the plasma present. The beam cyclotron instability can be excluded because of the required cold electrons $T_e < 3\, T_i$ and $T_i \approx T_n$. The ion acoustic instability possesses linear growth rates of a few percent of the ion plasma frequency, whereas the modified two stream instability growth rate corresponds to the lower hybrid frequency [18]. Therefore in the parameter range investigated the latter instability, which also has been noted by other authors [15, 6] as a possible source of electron heating in critically rotating plasma, turns out to be dominant.

Turbulent Heating and Conductivity

It is a peculiarity of the modified two stream instability that approximately equal electron and ion heating occurs [19], whereby due to the presence of a magnetic field an amount of energy determined by the ion mass $\frac{1}{2}\, m_i\, v_{cr}^2$ can be thermalized. We expect the high energy electrons which are responsible for the ionization to originate in this process of turbulent heating.

For the saturation stage of this instability an effective collision frequency is given [19]

$$\nu_{eff} = 0.2\, (m_e/m_i)^{1/2}\, \omega_{ce}\,. \qquad (3.9)$$

Using this collision frequency we obtain with regard to $\nu_{eff}^2 \gg \omega_{ce}^2$ an electron conductivity

$$\sigma_e = n_e\, e^2/m_e\, \nu_{eff} = 5\, (m_e/m_i)^{1/2}\, n_e\, e/B \qquad (3.10)$$

which predicts the experimentally found relation

$$j = \sigma\, E = \sigma\, v_{cr}\, B$$

$$\text{i.e. } j = \text{const}\, n_e \qquad (3.11)$$

(see Section II, 5.) as well as the right magnitude.

Spoke Structure

In the model presented above the plasma on the one hand exhibits an azimuthal $E \times B$ drift on the electrons but on the other hand the effective collision frequency caused by the instability just enables a radial electron current to flow which is comparable to the ion current. These contradictory properties of the electrons are incompatible in a spatially homogeneous model. The azimuthal density structure found experimentally suggests a separation of these properties in space.

In the front of the spoke, which is characterized by a steep increase of electron density (zone 1 in Fig. 8), we localize the turbulent electron heating due to the two stream instability. In this region the electron current carried by the newly formed electrons must flow.

Zone 2 is characterized by the decaying plasma of zone 1. Here the ions being produced in zone 1 are transported away radially whereas the electrons undergo the $E \times B$ drift almost without collisions and move with the spoke. In this way the instability which becomes effective in zone 1 is already being prepared here. In this practically extrinsically generated plasma of zone 2 the classical heat balance of the electrons can be applied. From Eq. (3.7) and the $\varkappa_e(T_e)$ curve given by Lehnert [13] for $E/B = v_{cr}$ a temperature $T_e = 3.8$ eV results which in addition turns out to be independent of the neutral gas pressure. This value and dependence is to a great degree confirmed by the experiment which gives the temperature in the density maxima corresponding to zone 2.

Summary

The original conception of a homogeneous critically rotating plasma turns out to be untenable on account of the experimental results presented. Indeed concrete indications have been found that indicate that the azimuthal structure detected by electrical and magnetic probes is causally connected to the critical velocity phenomenon under discussion. Independent of the voltage limitation the occurrence of the critical velocity has been proved by measuring the velocity of propagation of the rotating current spokes.

The local measurements of electron density and temperature which have been investigated for the first time in this paper demand a spatial separation of different processes. It is especially the rapid ionization which is connected to the critical velocity phenomenon that has been localized to the front of the current spokes. From this point of view a unique description of topologically different devices [20, 21] with critical velocity is obtainable in the "ionizing wave" concept. The particle balance based on the measured plasma parameters emphasizes the importance of turbulent heating for the rapid ionization. A detailled current balance requires a turbulent conductivity for the transport of electrons in a radial direction.

In detail it turned out that the turn-on conditions for the modified two stream instability are fulfilled. Further the growth rate of this instability exceeds those of all the other instabilities in magnetic fields. From this starting point some important steps have been made towards a final elucidation of the critical velocity phenomenon.

Moreover critical rotating plasmas will be of interest for subsequent investigations of turbulence aspects in magnetized plasmas. Within a wide range of parameters the quasistationary state of the homopolar plasma facilitates the investigation of experimental details.

Indeed the essentially unchanged spoke structure during the discharge period allows us to study the instability in the growth stage as well as in the transition to saturation.

Acknowledgements

We are grateful to Professor Dr. H. Schlüter for valuable discussion and encouragement in this work. The investigations are part of the joint efforts within the Sonderforschungsbereich 162 "Plasmaphysik Bochum/Jülich".

[1] U. V. Fahleson, Phys. Fluids **4**, 123 [1961].
[2] L. Danielsson, Astrophys. Space Sci. **24**, 459 [1973].
[3] H. Alfvén, On the Origin of the Solar System, Oxford Univ. Press 1954.
[4] L. Danielsson, Phys. Fluids **13**, 2288 [1970].
[5] J. C. Sherman, Astrophys. Space Sci. **24**, 487 [1973].
[6] M. A. Raadu, Trita-EPP-75-28 [1975].
[7] G. Himmel and A. Piel, J. Phys. D **6**, L108 [1973].
[8] A. R. Sherwood and W. B. Kunkel, J. Appl. Phys. **39**, 2348 [1968].
[9] B. Lehnert et al., Physica Scripta **9**, 53 [1974].
[10] J. G. Laframboise, UTIAS Rep. No. 100 [1965].
[11] G. Himmel and E. Möbius, Z. Naturforsch. **29 a**, 1572 [1974].
[12] B. Lehnert, Nucl. Fus. **11**, 485 [1971].
[13] B. Lehnert, Phys. Fluids **9**, 774 [1966].
[14] D. R. Bates et al., Proc. Roy. Soc. London **267 A**, 297 [1962].
[15] J. C. Sherman, J. Phys. B **7**, 244 [1974].
[16] N. A. Kervalishvili, ZHTF **45**, 811 [1975].
[17] C. N. Lashmore-Davis et al., Nucl. Fus. **13**, 193 [1973].
[18] M. Lampe et al., NRL Rep. 3076 [1975].
[19] O. Buneman, PL. Phys. **4**, 111 [1962].
[20] J. Eninger, Proc. 7th Int. Conf. Ioniz. Gases Belgrad; **1**, 520 [1965].
[21] I. Axnäs, TRITA-EPP-72-31 [1972].